A New Type of Macro-Elements for Efficient Two-Dimensional FEM Analysis

Grzegorz Fotyga, Krzysztof Nyka, *Member, IEEE*, and Lukasz Kulas, *Member, IEEE*

***Abstract*—This letter deals with a model order reduction technique applicable for driven and eigenvalue problems solved using the finite element method (FEM). It allows one to efficiently compute electromagnetic parameters of structures comprising small features that require strong local mesh refinement. The subdomains of very fine mesh are separated from the global domain as so called macro-elements that undergo model reduction. The macro-elements of reduced order are described by a significantly smaller number of unknowns, thus improving overall simulation speed. In addition, we present an algorithm of macro-elements multiple reuse, called cloning, which provides further decrease of the computation time and memory requirements. The results of the two numerical experiments, in which the local mesh refinement exceeds the factor of 400, illustrate the properties of the proposed methodology and prove that it increases the FEM efficiency significantly and is particularly suitable for multiscale problems with strong variations of desired mesh density.**

***Index Terms*—Finite element method (FEM), macro-element, macro-elements cloning, model order reduction (MOR).**

I. Introduction

THE FINITE element method (FEM) is one of the most powerful numerical techniques for solving a Maxwell equations system. It is widely known for its flexibility while analyzing arbitrarily shaped domain geometries and inhomogeneous materials. However, it requires long computational time, especially in multiscale problems.

One of the approaches to overcome this inconvenience was proposed in [1]. For FEM problems where local fine grids are necessary, it is suggested to use special macro-elements. Each macro-element captures the electromagnetic behavior of its entire region and has the form of a generalized impedance matrix (GIM). The GIM is frequency-dependent and describes the impedance relationship between electric and magnetic fields on the boundary of the macro-element. The advantage of incorporating such macro-elements is that they can be represented by a model of reduced order, thus limiting the number of unknowns to the number of boundary nodes. The reduced-order model of the GIM is obtained by means of the Passive Model Order Reduction Algorithm (PRIMA) [2]. The electromagnetic (EM) fields on the boundaries are expanded by global basis functions, and the nodes in the refined mesh are coupled with the outer (coarse) mesh via polynomial interpolation. The concept of macro-elements was also extensively investigated in the context of the finite-difference time domain (FDTD) and finite-difference frequency domain (FDFD) methods [3], [4]. In contrast to the method based on GIM, this allows one to analyze resonant cavities. This is due to the particular way in which the macromodels are incorporated into finite-difference equations, in which frequency-dependent terms are not introduced into the global matrix equations. As far as FEM is concerned, an interesting approach is presented in [5], where the computational domain is divided into many subdomains that are connected using an admittance matrix and can be analyzed independently. An approach that incorporates a reduced-order model of a feed network into efficient FEM simulation of an antenna array is presented in [6]. Other approaches are based on an interfacing finite-element grid with lumped networks in terms of admittance or impedance matrices and have been proposed in [7]–[9].

In this letter, an alternative implementation of macro-elements in FEM is proposed. The electromagnetic properties of regions that demand high mesh resolution are captured using macro-elements. However, instead of reducing the transfer function as in [1], the reduction is applied directly to the FEM equations in the manner similar to that proposed in [3] for the FDFD method, that is to say by projecting a chosen set of equations onto a smaller space spanned by orthonormal basis V. The basis is computed using the Efficient Nodal Order Reduction (ENOR) algorithm [10]. As a result, the global stiffness and mass matrices are free of any frequency-dependent elements, which means that this approach can be used to solve not only driven, but also eigenvalue, problems.

In comparison to [1], a different approach to provide transition between coarse and fine mesh on the boundary of macro-elements is proposed. From finite difference analysis, it is known that discontinuous meshes cause spatial frequency aliasing and phase velocity mismatch, which lead to spurious reflections [11]–[13]. Similar problems may also occur in finite element analysis. Instead of discontinuous mesh and polynomial interpolation, a layer of smooth mesh refinement is added, thus reducing the risk of spurious reflections from a macro-element border. Due to a different technique of incorporating the macro-elements into the global matrix and smooth transitions between the mesh inside and outside the macro-element, the new method appears to be more accurate than the method of [1]. The proposed algorithm allows one to incorporate many macro-elements within one computational domain, and what is more, one type of a macro-element can be used to compute the

Manuscript received February 01, 2011; revised March 08, 2011; accepted March 21, 2011. Date of publication April 05, 2011; date of current version April 14, 2011. This work was supported by the MNiSzW under Grant 5407/B/T02/2010/38).

The authors are with the Department of Electronics, Telecommunication and Informatics, WiComm Center of Excellence, The Gdańsk University of Technology, Gdańsk 80-255, Poland (e-mail: gfotyga@gmail.com; nyx@eti.pg.gda.pl; luke@eti.pg.gda.pl).

Digital Object Identifier 10.1109/LAWP.2011.2134063

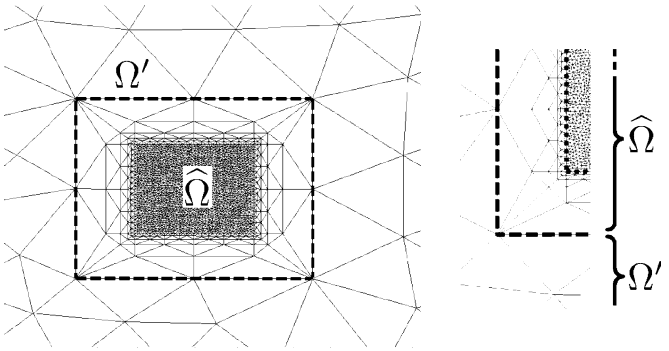

Fig. 1. *(left)* Two computational subdomains (separated by dashed line) of different discretization meshes. *(right)* Transition from coarse to fine mesh is in the refinement buffer layer between dashed and dotted lines.

electromagnetic properties of many identical areas. This operation, called macro-element cloning, reduces the computation time and memory requirements significantly.

II. Background

A. Finite Element Formulation

To illustrate the new technique of constructing and incorporating macro-elements, let us consider a simple case called in-plane propagation. Namely, we will analyze the E-polarized (TE) mode of wave propagation in an xy plane of a parallel-plane waveguide structure assuming homogeneity in the z-direction (transverse to the direction of propagation). For this arrangement, the two-dimensional wave equation can be written as

$$\nabla \cdot \left[\mu_r^{-1} \nabla \cdot E_z(x,y)\right] + k_0^2 \epsilon_r E_z(x,y) = f(x,y) \quad (1)$$

where $\epsilon_{\rm r}$ and $\mu_{\rm r}$ are the relative permittivity and permeability of the medium, respectively, k_0 is the wavenumber, and $f(x,y)$ is a source function. We impose Dirichlet homogeneous boundary conditions on the conducting surfaces, absorbing boundary conditions for the output port, and absorbing boundary conditions, together with the excitation for the input port.

A corresponding linear set of equations is obtained by discretizing the weak form of (1), employing Galerkin's method, assembling all element equations, and imposing boundary conditions [14], which leads to

$$(\mathbf{A} + k_0^2 \mathbf{B})\mathbf{e_z} = \mathbf{b} \quad (2)$$

where $\mathbf{b}$ is the excitation vector and $\mathbf{A}$, $\mathbf{B}$ are the stiffness and the mass matrix, respectively. Once the equation has been solved, the reflection and transmission coefficients can be calculated [14].

B. Model Order Reduction Technique

Let us assume that the computational domain Ω contains a region that requires much finer discretization. The operation of implementing a macro-element begins with dividing Ω into two subdomains (Fig. 1): Ω' containing K nodes with a coarse grid, and $\hat{\Omega}$ with L nodes and a refined grid. If consistent numbering of nodes in separate groups for Ω' and $\hat{\Omega}$ is used, the matrices $\mathbf{A}$ and $\mathbf{B}$ split into blocks $\mathbf{A'}$, $\mathbf{B'} \in R^{K\times K}$ and $\hat{\mathbf{A}}$, $\hat{\mathbf{B}} \in R^{L\times L}$, which correspond to the coarse and refined region, respectively. Nodes that lie on the boundary between Ω' and $\hat{\Omega}$ form four coupling matrices: $\mathbf{S}_A$, $\mathbf{S}_B \in R^{L\times K}$ and $\mathbf{S}_A^T$, $\mathbf{S}_B^T \in R^{K\times L}$

$$\left(\begin{bmatrix}\mathbf{A'} & \mathbf{S}_A^T \\ \mathbf{S}_A & \hat{\mathbf{A}}\end{bmatrix} + k_0^2 \begin{bmatrix}\mathbf{B'} & \mathbf{S}_B^T \\ \mathbf{S}_B & \hat{\mathbf{B}}\end{bmatrix}\right)\begin{bmatrix}\mathbf{e'_z} \\ \hat{\mathbf{e}}_\mathbf{z}\end{bmatrix} = \begin{bmatrix}\mathbf{b} \\ \mathbf{0}\end{bmatrix}. \quad (3)$$

In the approach presented here, it is assumed that the excitations are imposed outside of the macro-elements. After multiplication of (3), we obtain

$$\mathbf{A'e'_z} + \mathbf{S}_A^T \hat{\mathbf{e}}_\mathbf{z} + k_0^2 \mathbf{B'e'_z} + k_0^2 \mathbf{S}_B^T \hat{\mathbf{e}}_\mathbf{z} = \mathbf{b} \quad (4)$$

$$\mathbf{S}_A \mathbf{e'_z} + \hat{\mathbf{A}} \hat{\mathbf{e}}_\mathbf{z} = -k_0^2 \mathbf{S}_B \mathbf{e'_z} - k_0^2 \hat{\mathbf{B}} \hat{\mathbf{e}}_\mathbf{z}. \quad (5)$$

Equation (5) can be written as

$$(\hat{\mathbf{A}} + k_0^2 \hat{\mathbf{B}})\hat{\mathbf{e}}_\mathbf{z} = -(k_0^2 \mathbf{S}_B + \mathbf{S}_A)\mathbf{e'_z}. \quad (6)$$

After substituting $\mathbf{C} = \hat{\mathbf{B}}$, $\mathbf{\Gamma} = \hat{\mathbf{A}}$, $\mathbf{B}_e = -(s_0 \mathbf{S}_B + s_0^{-1} \mathbf{S}_A)$, and $s_0 = k_0$into (6), we obtain

$$\left(\mathbf{C}s_0 + \mathbf{\Gamma}\frac{1}{s_0}\right)\hat{\mathbf{e}}_\mathbf{z} = \mathbf{B}_e \mathbf{e'_z}. \quad (7)$$

The above form is amenable to model order reduction (MOR) using the ENOR algorithm [10]. It produces a set of orthonormal vectors forming an orthonormal basis $\mathbf{V} \in R^{L\times N}$ by matching block moments of the nodal values of the field, expanded about the selected frequency. N depends on the reduction order q and the number of nodes at the boundary between subdomains p (e.g., $p = 8$ in Fig. 1) and is equal to qp. As opposed to [1], there is no need to construct the frequency-dependent general impedance matrix because the basis $\mathbf{V}$ can be applied directly to the FEM equations (3) to project the equations inside the finely discretized region $\hat{\Omega}$. We will refer to such a reduced part as a macro-element that is described by matrices replacing the matrices $\hat{\mathbf{A}}$ and $\hat{\mathbf{B}}$ in (3)

$$\begin{bmatrix}\mathbf{A'} & \mathbf{S}_A^T\mathbf{V} \\ \mathbf{V}^T\mathbf{S}_A & \mathbf{V}^T\hat{\mathbf{A}}\mathbf{V}\end{bmatrix}\begin{bmatrix}\mathbf{e_z}' \\ \hat{\mathbf{e}}_\mathbf{zm}\end{bmatrix} + k_0^2 \begin{bmatrix}\mathbf{B'} & \mathbf{S}_B^T\mathbf{V} \\ \mathbf{V}^T\mathbf{S}_B & \mathbf{V}^T\hat{\mathbf{B}}\mathbf{V}\end{bmatrix}\begin{bmatrix}\mathbf{e'_z} \\ \hat{\mathbf{e}}_\mathbf{zm}\end{bmatrix} = \begin{bmatrix}\mathbf{b} \\ \mathbf{0}\end{bmatrix} \quad (8)$$

$$\hat{\mathbf{e}}_\mathbf{zm} = V^T \hat{\mathbf{e}}_\mathbf{z}. \quad (9)$$

The macro-element matrices $\mathbf{V}^T\hat{\mathbf{A}}\mathbf{V}$ and $\mathbf{V}^T\hat{\mathbf{B}}\mathbf{V} \in R^{N\times N}$ are of a much smaller size than $\hat{\mathbf{A}}$ and $\hat{\mathbf{B}}$ since $N << L$. However, they are dense. The accuracy of reduction depends on the number of reduced variables in the vector $\hat{\mathbf{e}}_\mathbf{zm}$, the structure inside the macro-element, and the reduction order q. It is worth mentioning that owing to the frequency-independent vectors V, there are also no frequency-dependent terms in the left-hand side matrices of (8). Thus, this approach can be employed in eigenvalue problems derived from (8) without the need of using nonlinear eigensolvers, which makes it an efficient method for analysis of resonators.

For the sake of simplicity, the formulation presented above refers to one macro-element embedded into the FEM grid. However, the proposed technique can be employed in many subdomains within one computational region. In such cases, the nodes should be numbered in the following order: $\Omega', \hat{\Omega}_1, \hat{\Omega}_2 \ldots \hat{\Omega}_N$.

In effect, an orthogonal basis $\mathbf{V}_n$ for each macro-element region can be computed using $\hat{\mathbf{A}}_n$, $\hat{\mathbf{B}}_n$ and appropriate coupling matrices $\mathbf{S}_{An}$ and $\mathbf{S}_{Bn}$.

C. Connecting Meshes Between Subdomains

Since the proposed technique is intended for the simulation of multiscale FEM problems, one of the main issues is to connect the nodes from the two regions: coarse Ω' and refined $\hat{\Omega}$. In [1], the EM fields on the boundary of the macro-element are expanded using polynomials in order to provide transition between meshes of different density. In effect, border nodes of the adjacent meshes do not have to coincide, but the polynomial interpolation can generate spurious reflections on the boundaries of macro-elements.

To avoid mesh discontinuity on the border of the macro-element, an interface of condensing mesh layer, called a buffer, is inserted. The buffer, shown in Fig. 1 between dashed and dotted lines, is considered an outer part of macro-element $\hat{\Omega}$. The coarse mesh in Ω' and the fine mesh of the inner region of $\hat{\Omega}$ can be irregular and generated independently before the buffer is added. For the sake of simplicity, we used only rectangular macro-elements, but the buffer can have any regular shape. To prevent excess regrowth of macro-elements, the buffer should be as narrow as possible. However, it is also important to avoid too narrow triangles in the buffer mesh because they could lead to ill-conditioned FEM matrices, which is a well-known property of FEM. The refinement algorithm that is used in the buffer is based on recursive bisection, which provides very rapid refinement of any high degree and allows for controlling the buffer width. For the example, in Fig. 1, the buffer width does not exceed the size of triangles of the coarse mesh. To check the immunity of the reduction algorithm to ill-conditioned matrices resulting from very narrow triangles in macro-element regions, we simulated the structure with the buffer layer of various widths. For the buffer as much as three times narrower than the one in Fig. 1, the reduction time increased by only 40%, whereas the solution error remained the same. It shows that the shape of triangles in the buffer is not critical.

In comparison to [1], this approach does not require interpolation between coarse and fine mesh, which makes it easier to implement and free from spurious reflection at the macro-element boundary.

D. Macro-Element Cloning

Let us consider a computational domain that contains many identical small areas, which is typical of, e.g., electromagnetic band-gap structures [15]. In such cases, the same fine mesh, buffer layer, and corresponding FEM matrices $\hat{\mathbf{A}}$ and $\hat{\mathbf{B}}$ can be used for each subdomain. This requires an equal number of nodes on each macro-element border, which can be forced during mesh generation. Therefore, one can generate the orthonormal basis $\mathbf{V}$, which is compatible with all subdomains. Moreover, after renumbering Ω' in such a way that the nodes at the boundaries surrounding each macro-element are numbered as last, identical coupling matrices $\mathbf{S_A}$ and $\mathbf{S_B}$ are generated for all macro-elements. Hence, only one reduction is required for all of the macro-elements. In other words, only one set of matrices—$\mathbf{V}^T\hat{\mathbf{A}}\mathbf{V}$, $\mathbf{V}^T\hat{\mathbf{B}}\mathbf{V}$, $\mathbf{V}^T\mathbf{S}_A$, and $\mathbf{V}^T\mathbf{S}_B$—has to be computed, stored, and used to capture the electromagnetic properties of all identical subdomains. This process is called macro-element cloning and provides considerable saving of simulation time and memory demand. In comparison to [1], where the matrix to be cloned is frequency-dependent GIM, the proposed cloning can be done once for the whole frequency range.

TABLE I
COMPARISON OF THE NUMERICAL RESULTS OF THE TRANSMISSION PROBLEM ANALYSIS FOR DIFFERENT REDUCTION ORDERS

q	Number of variables in macro-elements $(80N)$	Simulation time [s]	Reduction time [s]	maximum absolute error
2	1280	73.4	0.28	0.001
3	1920	77	0.47	2e-7
4	2560	82.6	0.79	1.5e-7
5	3200	85.3	1.21	1e-7

III. NUMERICAL RESULTS

We shall illustrate the proposed methodology through two numerical examples for driven and eigenvalue problems. All calculations were carried out on a computer with an Intel Core 2 Duo 6400 processor and 2 GB RAM.

The first case deals with an array of 8×10 dielectric posts with relative dielectric constant $\epsilon_{\mathrm{r}} = 50$, placed inside the waveguide uniform in the transverse direction (see [1] for details). In the FEM simulation, reflection and transmission coefficients were computed in 72 equidistant frequency points over the range of 15–30 GHz. First, a simulation for the problem without macro-elements was carried out in order to generate reference results for further tests concerning effects of macro-elements order reduction. For each of the 80 dielectric posts, 400:1 mesh refinement (increase of the number of nodes in the refined mesh) was applied, which resulted in 161 659 unknowns comprising as much as 156 640 nodes in all $\hat{\Omega}$ regions. The results are in very good agreement with the corresponding simulation in [1]. Then, the same structure was analyzed with 80 macro-elements of the size 0.3×0.3 mm^2 (covering the dielectric posts of the size 0.2×0.2 mm^2 each), incorporated into the standard FEM formulation. Since all dielectric loads are identical, for each reduction order we generated only one macro-element as well as one pair of coupling matrices $\mathbf{S_A}, \mathbf{S_B}$ and cloned them 79 times.

Table I compares the number of variables in all macro-elements $(80N)$, simulation time, reduction time, and maximum absolute error for the reduction order ranging from 2 to 5. It is clearly visible that the number of variables in refined regions is significantly reduced from more than 156 000 to as few as 1280 for q equal to 2. Also, the simulation time is reduced from 379.56 to less than 90 s, while the value of error is smaller than 0.001.

Fig. 2 shows frequency characteristics of transmission and reflection coefficients obtained from the following FEM simulations: one without macro-elements, and two simulations with macro-elements reduced using our method and the method presented in [1]. It can be noted that in the results from the analysis in [1], the error grows with the frequency, whereas in the method presented here, the results are almost indistinguishable

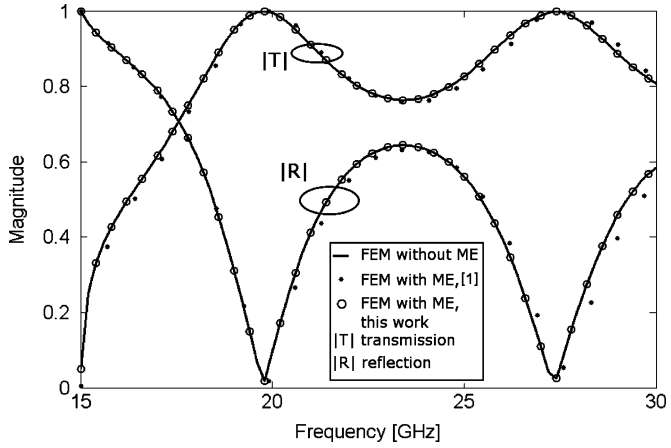

Fig. 2. Magnitude of the reflection and transmission coefficients versus frequency computed using the proposed reduction algorithm (FEM with ME, this letter) in comparison to the results obtained in [1] (FEM with ME, [1]) and the FEM algorithm without embedded macro-elements (FEM without ME).

TABLE II
COMPARISON OF THE NUMERICAL RESULTS OF THE EIGENVALUE PROBLEM ANALYSIS FOR DIFFERENT REDUCTION ORDERS

q	Simulation time [s]	maximum relative error [%]
2	0.56	0.045
3	0.59	4.2e-6
4	0.68	2.9e-6
5	0.82	2.1e-6

from the reference simulation without macro-elements over the entire frequency range.

The second numerical example is a 2-D resonator of the size 11×10 mm^2 made from a previously analyzed waveguide, closed by metallic walls. For this problem, the resonant frequencies of the first five eigenmodes in the structure are calculated using the Implicitly Restarted Arnoldi Method (IRAM). First, the simulations without macro-elements were carried out, and these results served as a reference. Since the number of variables within macro-elements and the time of their implementation are the same as in the first example, we present only the values of maximum relative error and computation time (Table II). The simulation time for the case without macro-elements is 13.9 s, which means that incorporation of macro-elements results in accelerating simulations from 17 to 25 times, depending on the reduction order q.

It is seen that q equal or greater than 4 does not significantly improve simulation accuracy, but only increases the numerical effort and computation time. Hence, in two presented examples, the most suitable value of q is 3.

IV. CONCLUSION

A new model order reduction technique applicable for the finite element method, based on the ENOR algorithm, has been presented in this letter. The examples discussed demonstrate the validity of the technique over the desired frequency range and prove that utilizing the proposed approach results in major reduction of the simulation time and the number of variables, both in driven and eigenvalue problems. In comparison to the FEM order reduction based on a general impedance matrix (GIM), our method exhibits better accuracy owing to unreflective transition between coarse mesh and strongly refined macro-elements. Another advantage over the GIM order reduction is the lack of frequency dependence of the reduced matrices. In order to further improve simulation efficiency, we have incorporated an algorithm of frequency-independent macro-element cloning. Our study is limited to two-dimensional space and nodal finite elements, but with further improvements, it can be directly extended into three-dimensional vector formulation.

REFERENCES

[1] Y. Zhu and A. C. Cangellaris, "Macro-elements for efficient FEM simulation of small geometric features in waveguide components," *IEEE Trans. Microw. Theory Tech.*, vol. 48, no. 12, pp. 2254–2260, Dec. 2000.

[2] A. Odabasioglu, M. Celik, and L. T. Pileggi, "PRIMA: Passive reduced order interconnect macromodeling algorithm," *IEEE Trans. Comput.-Aided Design*, vol. 17, pp. 645–653, Aug. 1998.

[3] L. Kulas and M. Mrozowski, "Macromodels in the frequency domain analysis of microwave resonators," *IEEE Microw. Wireless Compon. Lett.*, vol. 14, no. 3, pp. 94–96, Mar. 2004.

[4] B. Denecker, F. Olyslager, L. Knockaert, and D. de Zutter, "Automatic generation of subdomain models in 2D FDTD using reduced order modeling," *IEEE Microw. Guided Wave Lett.*, vol. 10, no. 8, pp. 301–303, Aug. 2000.

[5] V. de la Rubia and J. Zapata, "Microwave circuit design by means of direct decomposition in the finite-element method," *IEEE Trans. Microw. Theory Tech.*, vol. 55, no. 7, pp. 1520–1530, Jul. 2007.

[6] R. Wang, H. Wu, A. C. Cangellaris, and J. M. Jin, "Incorporation of feed-network modeling into the time-domain finite element analysis of antennas," in *Proc. IEEE Antennas Propag. Soc. Int. Symp.*, Honolulu, HI, Jun. 9–15, 2007, pp. 3520–3523.

[7] H. Wu and A. C. Cangellaris, "Model-Order reduction of finite-element approximations of passive electromagnetic devices including lumped electrical-circuit models," *IEEE Trans. Microw. Theory Tech.*, vol. 52, no. 9, pp. 2305–2313, Sep. 2004.

[8] R. Wang and J. M. Jin, "Incorporation of multiport lumped networks into the hybrid time-domain finite-element analysis," *IEEE Trans. Microw. Theory Tech.*, vol. 57, no. 8, pp. 2030–2037, Aug. 2009.

[9] S.-H. Lee and J. M. Jin, "Fast reduced-order finite-element modeling of lossy thin wires using lumped impedance elements," *IEEE Trans. Adv. Packag.*, vol. 33, no. 1, pp. 212–218, Feb. 2010.

[10] B. N. Sheehan, "ENOR: Model order reduction of RLC circuits using nodal equations for efficient factorization," in *Proc. 36th Design Autom. Conf.*, New Orleans, LA, 1999, pp. 17–21.

[11] B. Donderici and F. L. Teixeira, "Improved FDTD subgridding algorithms via digital filtering and domain overriding," *IEEE Trans. Antennas Propag.*, vol. 53, no. 9, pp. 2938–2951, Sep. 2005.

[12] L. Kulas and M. Mrozowski, "Low-reflection subgridding," *IEEE Trans. Microw. Theory Tech.*, vol. 53, no. 5, pp. 1587–1592, May 2005.

[13] B. Donderici and F. L. Teixeira, "Accurate interfacing of heterogeneous structured FDTD grid components," *IEEE Trans. Antennas Propag.*, vol. 54, no. 6, pp. 1826–1835, Jun. 2006.

[14] J. M. Jin, *The Finite Element Method in Electromagnetics*, 2nd ed. New York: IEEE Press, 2002.

[15] M. E. de Cos, Yu. Alvarez, R. C. Hadarig, and F. Las-Heras, "Novel SHF-Band uniplanar artificial magnetic conductor," *IEEE Antennas Wireless Propag. Lett.*, vol. 9, pp. 44–47, 2010.